Methodology

Two separate temperature perturbations are examined to study both near- and long-term effects of climate change on air quality. Temperature increases of 1 °C and 3 °C are considered as separate perturbation scenarios so that the effect of temperature on air quality can be analyzed in detail. Changes to temperature are applied uniformly across the model domain for all times of day and week. The magnitude of the temperature perturbations for both the LTEMP and HTEMP cases are in harmony with several climate studies. An early regional climate modeling study by Snyder et al. (2002) found temperature increases of 1.4 °C – 3.8 °C across California under 2 x CO₂ conditions. Another regional study by Hayhoe et al. (2004) examined a range of potential future climates in California and indicated mid-century (2020-2049) and end-of-century (2070-2099) summer temperature increases of 1.2 °C – 1.4 °C and 2.15 °C – 4.1 °C, respectively. These climate projections were based on the lowest and highest Intergovernmental Panel on Climate Change (IPCC) emissions pathways utilizing the low sensitivity Parallel Climate Model (PCM). The mid-century temperature increases projected by Hayhoe et al. (2004) are consistent with results from Zhao et al. (2011b) who showed a summertime temperature rise of 1.5 K over inland portions of California, with slightly lower increases over the neighboring Pacific Ocean for the years 2047-2053. Using an ensemble of 15 global climate models and a doubled CO₂ scenario, Coquard et al. (2004) showed model-averaged temperature increases of 2.5 K – 2.8 K over the Western United States during the warm season (June to October). Overall, both global and regional studies for a doubled CO₂ atmosphere indicate temperature increases in the 2°C – 3°C range over the western United States, with increases as high as 3.8 °C in California (Steiner et al., 2006). In addition to the temperature dependence of chemical reaction rates in the model, high temperatures favor the decomposition of PAN, increasing NO_X, an important ozone

precursor (Carreras-Sospedra et al. 2006). The partitioning of species into the aerosol phase is also temperature dependent due to changes in volatility. In order to isolate the effect of temperature increases on atmospheric chemistry processes, changes in anthropogenic emissions and other meteorological variables typically associated with higher temperatures such as sunny skies, stagnation, or changes in mixing depth are not considered in the temperature perturbation scenarios. This is the same approach used for temperature perturbation scenarios in other regional air quality modeling studies (Aw and Kleeman, 2003; Steiner et al., 2006; Kleeman, 2008; Millstein and Harley, 2009). Therefore, the temperature only perturbation scenarios represent a lower limit for the impact of increasing temperatures on air quality.

The approach for perturbations to absolute humidity is based on the assumption that relative humidity will remain approximately constant in the future climate. This is the same approach used by many other model perturbation analyses for southern California (Aw and Kleeman, 2003; Steiner et al., 2006; Millstein and Harley, 2009). Absolute humidity values are increased in accordance with an assumed temperature increase of 3 °C. First, the relative humidity is calculated at the base case temperature and absolute humidity values for each computational cell in the model at each hour of day. Then, holding the relative humidity constant, the new (perturbed) values of absolute humidity are calculated based on the new (increased) temperature values. Although the increase in absolute humidity is based on the increase in temperature, perturbations to absolute humidity are considered separately from increases to temperature and other meteorological variables in the HUMID scenario. In this scenario, both absolute and relative humidity increase while temperature values remain equal to those of the base case. In contrast, the scenarios that combine the HTEMP and HUMID

perturbations include increases to both temperature and absolute humidity such that the relative humidity remains the same as in the base case.

Perturbations to biogenic emissions of isoprene were also considered as a separate case. While biogenic emissions of isoprene are sensitive to both temperature and light, increases here are based on a temperature increase of 3 °C. Emissions of isoprene are observed to increase exponentially with leaf temperatures less than 30 °C, and continue to increase with increasing temperature until saturation at temperatures above 40 °C (Guenther et al., 1993). The average increase in isoprene emissions used in this study is 60%, based on base case model temperature values and a temperature increase of +3 °C in the future climate. Three studies reviewed by Guenther et al. (2006) that examine the response of isoprene emissions to potential future climate scenarios predicted a 35% to 70% increase in isoprene emissions associated with increased temperatures. It is noted that the increase in isoprene emissions associated with future climate change is highly dependent on the model and scenario utilized; see Guenther et al. (2006) for further details. In BIO scenario, only biogenic emissions are increased while all other meteorological variables remained unchanged from the base case, isolating the effects of increased biogenic isoprene emissions on air quality.

Changes in global climate and emissions also influence boundary conditions through changes in the background concentrations of different chemical species. Therefore, the impact of perturbing boundary conditions at the western inflow is examined in the BC scenario. The presence of strong sea-breeze effects in the SoCAB results in a predominant wind direction of northeast, transporting air parcels inland from the Pacific Ocean. Therefore, only boundary conditions along the western edge of the domain are perturbed in the BC scenario, while the boundary conditions for all other (North, South, and East) sides remain unchanged from base

case levels. Early studies by Vingarzan (2004) and Ebi and McGregor (2008) predicted that surface ozone background concentrations will reach at least 60 ppb by the years 2050–2060. A more recent study by Brown-Steiner and Hess (2011) examined the influence of Asian emissions on surface ozone concentrations in the United States. They reported that seasonally averaged ozone mixing ratios in the boundary layer for the Western United States are in the 63.6 ± 8.4 ppb range for JJA. Several modeling studies have examined the impact of changes in the background concentration or boundary conditions for a variety of species on air quality in California (Steiner et al., 2006; Kleeman, 2008; Millstein and Harley, 2009). Steiner et al. (2006) estimated a 30% increase in ozone concentrations (30 ppb to 40 ppb) at the western inflow for the year 2050 based upon contributions from both an increase in global background ozone and ozone reaching the Pacific coast from Asian emissions. Steiner et al. (2006) also increased western boundary conditions for CO from 80 ppb to 104 ppb (a 30% increase) but held NO and NO₂ at 1 ppb for both the base case and perturbation scenario as this value is already considered to be a large amount of NO_X entering the domain. Millstein and Harley (2009) utilized a 30% increase in ozone and CO boundary conditions at the western boundary for California following Steiner et al. (2006). Kleeman (2008) used boundary conditions of O₃, CO, NO, and NO₂ of 30 ppb, 200 ppb, 1 ppb, and 1 ppb, respectively, for the California study domain. Although a boundary condition perturbation scenario was not considered, Kleeman (2008) evaluated the impact of increasing background ozone concentrations from 30 ppb to 60 ppb based on long-term O₃ trends and predictions for the next 50 to 100 years. In the present study, western inflow boundary conditions of ozone are increased from 40 ppb in the base case to 55 ppb in the BC scenario, representing an approximate 30% increase as suggested by Steiner et al. (2006) and Millstein and Harley (2009). This level of ozone entering the domain is in line with both global and regional

studies that suggested surface ozone background concentrations will be in the 60 ppb range by midcentury (Vingarzan, 2004; Ebi and McGregor, 2008; Kleeman, 2008; Brown-Steiner and Hess, 2011). Western boundary conditions of NO and NO₂ are increased from 0.3 ppb and 0.5 ppb in the base case to 1 ppb and 1 ppb in the BC scenario to be in line with Steiner et al. (2006) and Kleeman (2008). The chosen boundary conditions for NO_X represent an upper limit to those expected to occur in the future. Boundary conditions for CO are held constant at 120 ppb for all model runs. This value falls between that used by Steiner et al. (2006) and Kleeman (2007).

In addition to considering all perturbations separately to isolate the effects of each individual parameter, various combinations of the described perturbations were also considered to gain insight into the influence of future meteorological conditions on ozone, PM, and SOA concentrations. For example, increased temperatures, increased absolute humidity (such that relative humidity remains constant), and increased biogenic emissions of isoprene were considered together in the HTEMP+HUMID+BIO scenario for a combined climate change effect. Adding to this scenario expected future changes in anthropogenic emissions for the year 2023 and changes in western boundary conditions due to long range transport from Asia results in the HTEMP+HUMID+BIO+BC scenario. This scenario considers all perturbations simultaneously and provides a comprehensive assessment of future air quality in the SoCAB. Due to the nonlinearity of air pollution dynamics and the competing and compounding effects of these perturbations, consideration of different combinations of the perturbations is essential to understand the sensitivity of pollutant concentrations to climate change.

There are several different forms available to visualize data and report results from model runs that are described briefly here. Output data for each perturbation scenario is compared to the base case that uses the same emissions inventory and is presented in a variety of tables and

figures to illustrate the impacts of climate change on air quality for different spatial and temporal scales. Tables of results allow for concise quantitative presentation of output data and are presented on a domain wide average basis as well as at key individual locations within the domain. Domain wide averages are calculated by averaging the concentration of the given pollutant for all computational cells in the domain and provide a single number representing the overall effect of a perturbation scenario on regional air quality. On the other hand, examination of peak pollutant concentrations at select individual locations provides insight into the sensitivity of pollutant formation to the variety of different microclimates found within the SoCAB. Data in all tables are shown for 16:00 h (4:00pm) local time (LT), the time of day when ozone concentrations are typically at a maximum. Although PM concentrations typically peak during the early morning hours, the largest *changes* in PM and SOA concentrations occur during the afternoon hours. In addition to the tables of quantitative data, delta contour plots that encompass the entire domain are generated on two different timescales for graphical representation of changes in the ground-level concentration of a specific species for a perturbation scenario versus the base case. The contour plots generated at 16:00 h LT show changes in the peak one-hour average concentration for the chosen species and perturbation scenario and are included to supplement data presented in the aforementioned tables. The 24-hour average delta contour plots, which average the change in concentration of a particular species for the entire day of simulation, provide another look at the overall impact of a perturbation on regional air quality. Thus, while domain wide average values presented in the form of tables are spatially averaged values at a specific time of day, 24-hour average delta contour plots are temporally averaged values presented graphically for all locations in the domain. Both examine the average, overall effect of the specified perturbation scenario on pollutant concentrations for the entire domain. These 24hour average contours capture both daytime and nighttime influences on changes in pollutant concentrations, an important consideration for ozone and other pollutants whose concentrations are governed by photochemical processes. Concentration data in both the tables and the figures is presented for the bottom layer of the modeling domain, representative of ground level.

Table S1Total domain-wide anthropogenic emissions (tons/day) for key precursor species in the 2005 and controlled 2023 emissions inventories used in this study.

Species	2005 Emissions	2023 Emissions
CO	4082.1	2350.6
HCHO	19.7	10.2
NH_3	165.4	166.6
NO	622.1	182.0
NO_2	108.4	31.1
SO_2	86.7	27.8

Results

Table S2Domain wide averages at 16:00h LT using 2005 emissions. Base case levels shown in top row. Difference and percent difference in concentration between the specified perturbation scenario and the base case shown in bottom rows. Positive values represent increases in concentration with respect to the base case. The dash (--) indicates that the difference is less than the number of significant figures shown (i.e., less than 0.1 change from base case levels).

Base Case	O ₃ (ppb)	PM ₁₀ (μg/m ³) 49	PM _{2.5} (μg/m ³) 34	SOA (μg/m³) 4.1
LTEMP	3.1, 3.3%	-0.9, -1.9%	-0.7, -2.1%	-0.3, -6.7%
HTEMP	9.0, 9.7%	-2.9, -5.9%	-2.2, -6.5%	-0.8,-20.0%
HUMID	1.0, 1.1%	0.4, 0.9%	0.3, 1.0%	0.1, 3.2%
BIO	1.2, 1.3%			
HTEMP+HUMID	10.6, 11.4%	-2.4, -4.9%	-1.8, -5.2%	-0.7,-17.2%
HTEMP+BIO	10.3, 11.1%	-2.8, -5.8%	-2.1, -6.3%	-0.8,-19.2%
HTEMP+HUMID+BIO	11.8, 12.7%	-2.4, -4.8%	-1.8, -5.2%	-0.7,-16.4%
BC	4.5, 4.8%	0.3, 0.7%	0.2, 0.5%	
HTEMP+HUMID+BIO+BC	16.6, 17.8%	-2.0, -4.1%	-1.5, -4.5%	-0.6,-15.5%

Table S3 PM_{2.5} concentration (μ g/m³) for select locations at 16:00h LT using 2023 emissions. Base case levels shown in top row. Difference and percent difference in PM_{2.5} concentration between the specified perturbation scenario and the base case shown in bottom rows. Positive values represent increases in concentration with respect to the base case. The dash (--) indicates that the difference is less than the number of significant figures shown (i.e., less than 0.1 change from base case levels).

	Los Angeles	Riverside	Anaheim	Pomona	Newhall	Long Beach
Base Case PM _{2.5}	26	40	23	70	30	30
LTEMP	-0.4, -1.7%	-1.0, -2.5%	-0.4, -1.7%	-1.1, -1.5%	-0.7, -2.3%	-0.1, -0.2%
HTEMP	-0.8, -3.0%	-2.6, -6.5%	-0.5, -2.1%	-6.3, -9.0%	-1.4, -4.8%	-0.4, -1.3%
HUMID	0.1, 0.5%	0.5, 1.1%		1.8, 2.5%	-0.1, -0.5%	0.2, 0.8%
BIO		-0.1, -0.2%	-0.3, -1.1%		-0.4, -1.3%	-0.1, -0.3%
HTEMP+HUMID	-0.6, -2.2%	-2.3, -5.8%	-0.5, -2.0%	-4.3, -6.1%	-1.3, -4.3%	-0.1, -0.4%
HTEMP+BIO	-1.0, -3.6%	-2.8, -7.1%	-0.6, -2.5%	-4.3, -6.1%	-1.5, -5.1%	-0.4, -1.4%
HTEMP+HUMID+BIO	-0.7, -2.5%	-2.5, -6.2%	-0.7, -3.0%	-4.1, -5.9%	-1.5, -5.1%	-0.2, -0.6%
BC	0.3, 1.0%	0.5, 1.3%		0.4, 0.5%	0.5, 1.8%	0.4, 1.4%
HTEMP+HUMID+BIO+BC	-0.3, -1.3%	-2.6, -6.5%		-4.5, -6.4%	-0.9, -2.9%	0.5, 1.8%

Table S4 PM_{2.5} concentration (μ g/m³) for select locations at 16:00h LT using 2005 emissions. Base case levels shown in top row. Difference and percent difference in PM_{2.5} concentration between the specified perturbation scenario and the base case shown in bottom rows. Positive values represent increases in concentration with respect to the base case. The dash (--) indicates that the difference is less than the number of significant figures shown (i.e., less than 0.1 change from base case levels).

	Los Angeles	Riverside	Anaheim	Pomona	Newhall	Long Beach
Base Case PM _{2.5}	28	56	25	72	39	23
LTEMP	0.2, 0.9%	-2.2, -3.9%	-0.4, -1.8%	-1.7, -2.4%	-0.8, -2.1%	-0.1, -0.4%
HTEMP	-0.9, -3.2%	-4.3, -7.7%	-1.1, -4.5%	-4.5, -6.2%	-3.1, -8.0%	-0.2, -0.8%
HUMID	0.8, 2.9%	0.4, 0.8%	0.3, 1.2%	0.1, 0.1%	1.0, 2.6%	0.6, 2.8%
BIO	0.3, 1.1%	0.9, 1.6%		-0.5, -0.6%	0.3, 0.8%	0.4, 1.6%
HTEMP+HUMID	-0.1, -0.3%	-4.1, -7.4%	-0.6, -2.5%	-4.3, -6.0%	-2.5, -6.5%	-0.2, -1.0%
HTEMP+BIO	-0.8, -3.0%	-4.7, -8.4%	-0.9, -3.8%	-4.1, -5.7%	-3.0, -7.7%	-0.4, -1.9%
HTEMP+HUMID+BIO	-0.7, -2.7%	-4.1, -7.3%	-0.7, -2.8%	-4.3, -6.0%	-2.4, -6.2%	-0.2, -0.9%
BC	0.9, 3.3%	0.9, 1.6%	0.6, 2.4%	-0.4, -0.5%	0.9, 2.2%	1.1, 4.9%
HTEMP+HUMID+BIO+BC	-0.1, -0.5%	-3.2, -5.8%		-4.3, -6.0%	-1.4, -3.6%	1.0, 4.3%

Table S5 PM $_{10}$ concentration (µg/m 3) for select locations at 16:00h LT using 2005 emissions: Base case levels shown in top row. Difference and percent difference in PM $_{10}$ concentration between the specified perturbation scenario and the base case shown in bottom rows. Positive values represent increases in concentration with respect to the base case. The dash (--) indicates that the difference is less than the number of significant figures shown (i.e., less than 0.1 change from base case levels).

Base Case PM ₁₀	Los Angeles 33	Riverside 96	Anaheim 32	Pomona 96	Newhall 66	Long Beach 29
LTEMP	0.3, 0.8%	-1.7, -1.8%	-0.3, -0.8%	-1.5, -1.5%	-1.1, -1.7%	
HTEMP	-0.9, -2.6%	-5.4, -5.6%	-1.0, -3.2%	-4.8, -5.0%	-4.7, -7.1%	-0.1, -0.2%
HUMID	0.9, 2.6%	1.4, 1.5%	0.4, 1.2%	0.3, 0.3%	1.3, 1.9%	0.7, 2.3%
BIO	0.3, 1.0%	1.4, 1.5%	0.1, 0.3%	-0.3, -0.3%	-0.8, -1.2%	0.4, 1.4%
HTEMP+HUMID		-4.2, -4.4%	-0.5, -1.7%	-4.0, -4.1%	-4.2, -6.3%	-0.1, -0.2%
HTEMP+BIO	-0.8, -2.4%	-5.5, -5.8%	-0.8, -2.6%	-4.4, -4.6%	-4.4, -6.7%	-0.3, -1.1%
HTEMP+HUMID+BIO	-0.6, -1.9%	-4.4, -4.6%	-0.5, -1.7%	-4.0, -4.2%	-4.0, -6.0%	-0.1, -0.3%
BC	1.0, 2.8%	1.0, 1.0%	0.9, 2.8%	-0.1, -0.1%	1.8, 2.8%	1.3, 4.4%
HTEMP+HUMID+BIO+BC		-3.4, -3.6%	0.2, 0.7%	-3.9, -4.0%	-2.5, -3.7%	1.3, 4.7%

Table S6 SOA concentration ($\mu g/m^3$) for select locations at 16:00h LT using 2005 emissions. Base case levels shown in top row. Difference and percent difference in SOA concentration between the specified perturbation scenario and the base case shown in bottom rows. Positive values represent increases in concentration with respect to the base case. The dash (--) indicates that the difference is less than the number of significant figures shown (i.e., less than 0.1 change from base case levels).

	Los Angeles	Riverside	Anaheim	Pomona	Newhall	Long Beach
Base Case SOA	2.6	11.0	1.3	9.2	6.0	0.7
LTEMP	-0.2, -6.6%	-0.7, -6.5%	-0.1, -4.4%	-0.5, -5.1%	-0.3, -5.6%	
HTEMP	-0.5, -17.6%	-2.3, -20.8%	-0.2, -16.2%	-1.6, -17.0%	-1.2, -19.5%	-0.1, -19.6%
HUMID	0.1, 5.7%	0.3, 2.8%		0.4, 4.1%	0.1, 1.1%	
BIO						
HTEMP+HUMID	-0.3, -12.2%	-2.0, -18.5%	-0.1, -10.4%	-1.2, -13.0%	-1.0, -17.3%	-0.1, -14.6%
HTEMP+BIO	-0.5, -17.7%	-2.3, -20.7%	-0.2, -15.7%	-1.5, -16.5%	-1.0, -16.6%	-0.1, -18.8%
HTEMP+HUMID+BIO	-0.3, -12.4%	-2.0, -18.2%	-0.1, -9.1%	-1.2, -13.1%	-1.0, -15.9%	-0.1, -15.6%
BC		0.2, 2.0%		0.1, 0.6%	0.2, 4.1%	
HTEMP+HUMID+BIO+BC	-0.3, -9.7%	-1.9, -16.8%	-0.1, -6.4%	-1.1, -12.4%	-1.0, -16.2%	-0.1, -12.4%

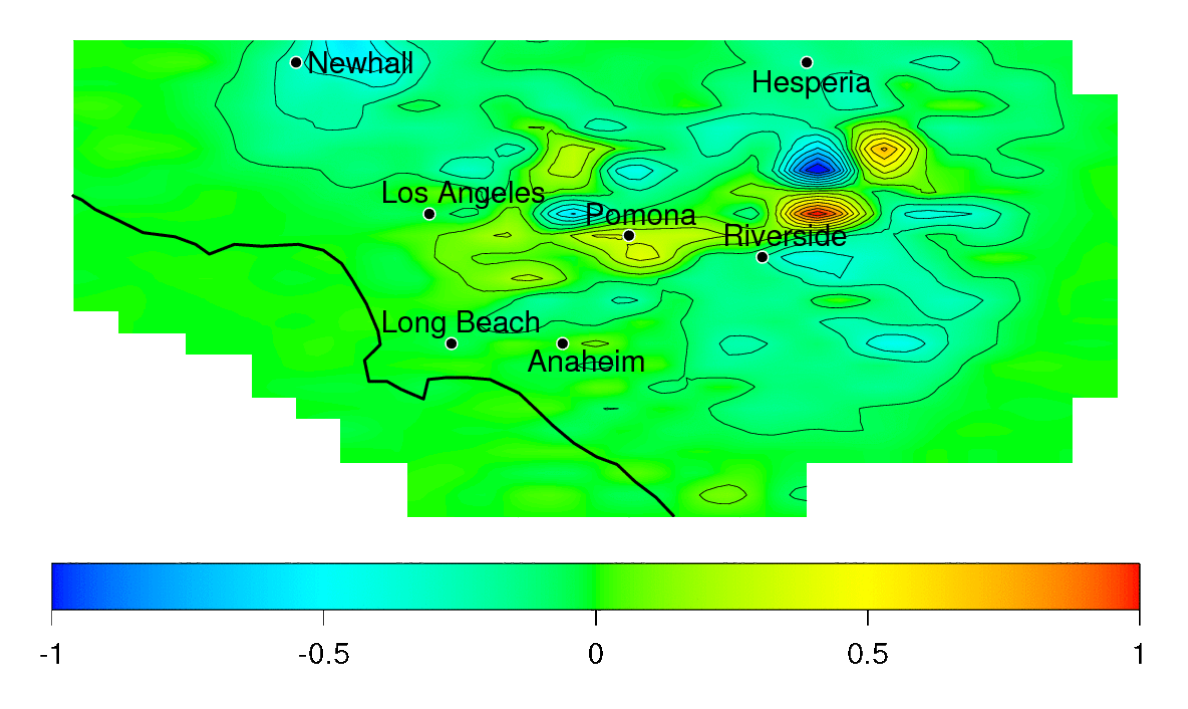
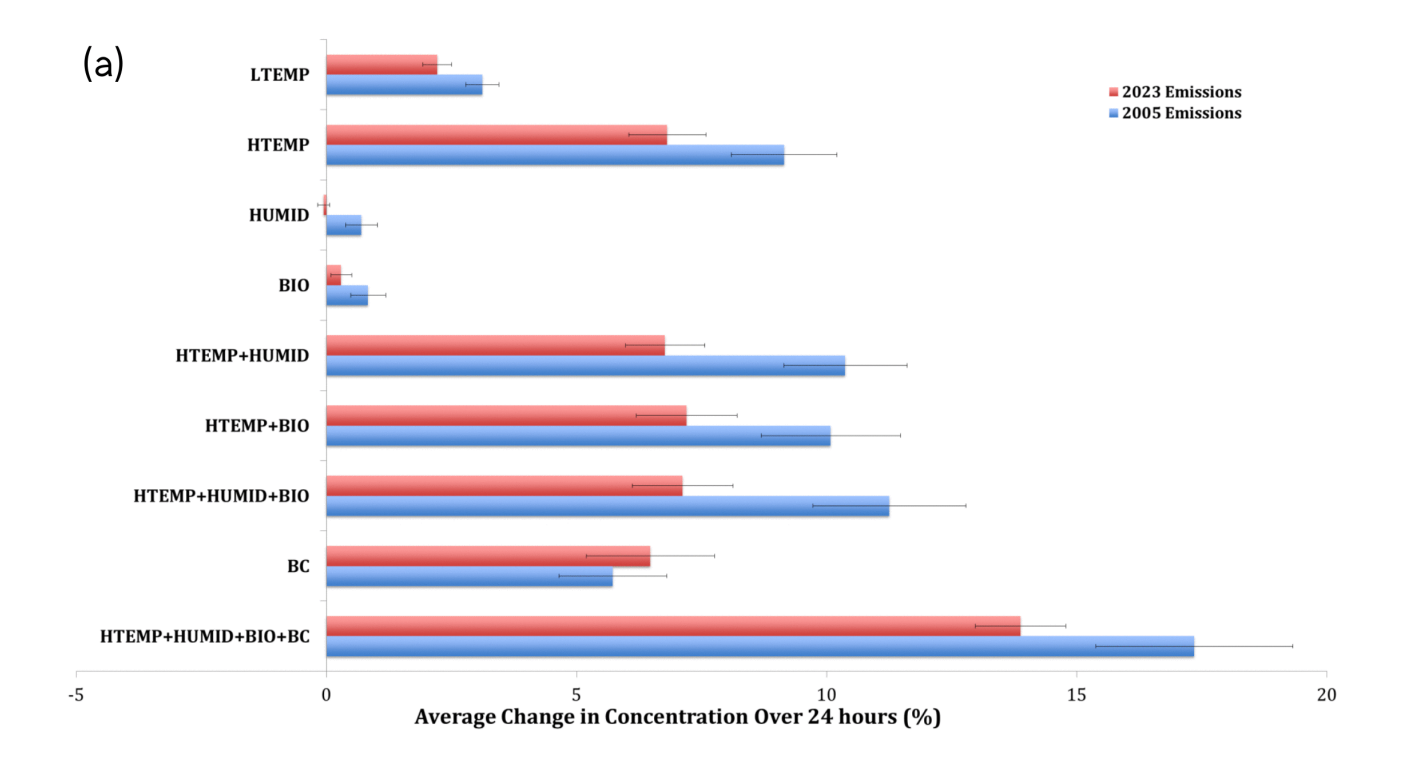


Figure S1: Differences between future and base case afternoon nitrate (NO_3) PM_{10} concentrations ($\mu g/m^3$) at 16:00 h in the BIO scenario when using 2023 emissions. Positive values represent increases in concentration with respect to the base case.



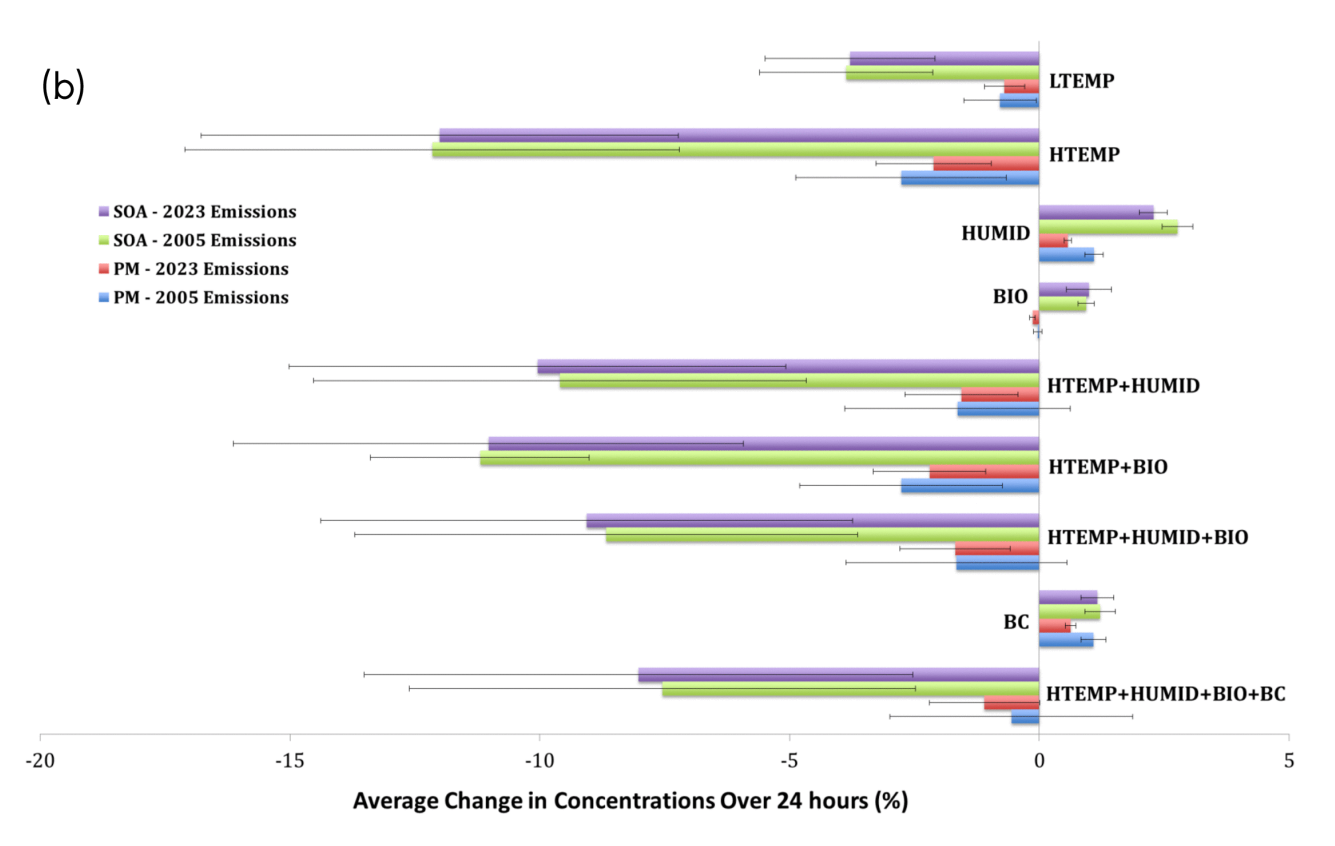


Figure S2: Relative changes in domain wide average concentrations of (a) ozone and (b) PM_{10} and SOA for each perturbation scenario in both emissions cases. Colored bars represent the average percentage change in concentration over 24-hours for the entire domain. Error bars indicate one standard deviation above or below the mean. Positive values represent increases in concentration with respect to the base case.

References

Aw, J., & Kleeman, M. J. (2003). Evaluating the first-order effect of intraannual temperature variability on urban air pollution. *Journal of Geophysical Research: Atmospheres (1984–2012), 108*(D12).

Brown-Steiner, B., & Hess, P. (2011). Asian influence on surface ozone in the United States: A comparison of chemistry, seasonality, and transport mechanisms. *Journal of Geophysical Research: Atmospheres* (1984–2012),116(D17).

Carreras-Sospedra, M., Dabdub, D., Rodriguez, M., & Brouwer, J. (2006). Air quality modeling in the south coast air basin of California: What do the numbers really mean?. *Journal of the Air & Waste Management Association*, *56*(8), 1184-1195.

Coquard, J., Duffy, P. B., Taylor, K. E., & Iorio, J. P. (2004). Present and future surface climate in the western USA as simulated by 15 global climate models. *Climate Dynamics*, *23*(5), 455-472.

Ebi, K. L., & McGregor, G. (2008). Climate change, tropospheric ozone and particulate matter, and health impacts. *Environ Health Perspect*, *116*(11), 1449-1455.

Guenther, A. B., Zimmerman, P. R., Harley, P. C., Monson, R. K., & Fall, R. (1993). Isoprene and monoterpene emission rate variability: model evaluations and sensitivity analyses. *Journal of Geophysical Research: Atmospheres (1984–2012)*, *98*(D7), 12609-12617.

Guenther, A., Karl, T., Harley, P., Wiedinmyer, C., Palmer, P. I., & Geron, C. (2006). Estimates of global terrestrial isoprene emissions using MEGAN (Model of Emissions of Gases and Aerosols from Nature). *Atmospheric Chemistry and Physics Discussions*, *6*(1), 107-173.

Hayhoe, K., Cayan, D., Field, C.B., Frumhoff, P.C., Maurer, E.P., Miller, N.L., Moser, S.C., Schneider, S.H., Cahill, K.N., Cleland, E.E. and Dale, L., (2004). Emissions pathways, climate change, and impacts on California. *Proceedings of the National Academy of Sciences of the United States of America*, 101(34), 12422-12427.

Kleeman, M. J. (2008). A preliminary assessment of the sensitivity of air quality in California to global change. *Climatic Change*, 87(1), 273-292.

Millstein, D. E., & Harley, R. A. (2009). Impact of climate change on photochemical air pollution in Southern California. *Atmospheric Chemistry and Physics*, *9*(11), 3745-3754.

Snyder, M. A., Bell, J. L., Sloan, L. C., Duffy, P. B., & Govindasamy, B. (2002). Climate responses to a doubling of atmospheric carbon dioxide for a climatically vulnerable region. *Geophysical Research Letters*, *29*(11), 9-1.

Steiner, A. L., Tonse, S., Cohen, R. C., Goldstein, A. H., & Harley, R. A. (2006). Influence of future climate and emissions on regional air quality in California. *Journal of Geophysical Research: Atmospheres* (1984–2012),111(D18).

Vingarzan, R. (2004). A review of surface ozone background levels and trends. *Atmospheric Environment*, 38(21), 3431-3442.

Zhao, Z., Chen, S. H., Kleeman, M. J., & Mahmud, A. (2011b). The impact of climate change on air quality-related meteorological conditions in California. Part II: Present versus future time simulation analysis. *Journal of climate*, 24(13), 3362-3376.